SciMedCentral

JSM Biotechnology & Biomedical Engineering

Short Communication

Myostatin Modulates the Heart Rate in Zebrafish Embryos

Dennise Lizárraga-Lizárraga[1], Ataúlfo Martínez-Torres[2], Raúl Llera-Herrera[3], Ángeles Edith Espino-Saldaña[2], and Alejandra García-Gasca[1]*

[1]*Centro de Investigación en Alimentación y Desarrollo (CIAD), Avenida Sábalo Cerritos s/n, Mexico*

[2]*Departamento de Neurobiología Celular y Molecular, Universidad Nacional Autónoma de México, Mexico*

[3]*Centro de Investigación en Alimentación y Desarrollo (CIAD), Avenida Sábalo Cerritos s/n, Mazatlán, Mexic*

***Corresponding author**

Alejandra Garcia-Gasca, Centro de Investigación en Alimentación y Desarrollo (CIAD), Laboratorio de Biología Molecular, Avenida Sábalo Cerritos s/n, Mazatlán, Sinaloa 82110, Mexico, Tel: 52-669-989-8700; Email: alegar@ciad.mx

Submitted: 21 April 2017

Accepted: 09 May 2017

Published: 10 May 2017

ISSN: 2333-7117

Keywords

- Myostatin
- Heart rate
- Zebrafish
- CRISPR/Cas9
- Muscle growth
- Embryo

Abstract

Myostatin, a negative regulator of skeletal muscle growth, is also expressed in cardiac muscle; however its function in this tissue is poorly understood. In this study, the CRISPR/Cas9 system was used to inactivate mstn in zebrafish. Microinjection was performed in one-cell stage embryos, and genomic DNA sequencing analysis confirmed high mutation efficiency. Coronal histological sections from 5 days post-fertilization (dpf) larvae showed the expected phenotype of skeletal muscle growth, but no evident morphological alterations were observed in the heart. An examination of 2 dpf embryos revealed a significant decrease in the heart rate, suggesting that mstn could play a role in cardiac function during development.

ABBREVIATIONS

mstn: Myostatin; dpf: Days post-fertilisation; PAM: Protospacer Adjacent Motif; NGS: Next Generation Sequencing

INTRODUCTION

Myostatin is a negative regulator of skeletal muscle growth [1]. In mammals, it is expressed in skeletal [2,3], cardiac [4], and smooth muscle [5]. The role of myostatin in cardiac muscle has not been completely elucidated [4,6-9]. Nevertheless, it has been observed that cardiac myostatin is induced during heart failure in different mammalian models producing skeletal muscle wasting [10,11], and that cardiac function improves in aging knockout mice [7], suggesting, on one hand, an inverse association between myostatin induction and heart performance and, on the other hand, a therapeutic potential of myostatin inactivation to improve cardiac function and alleviate skeletal muscle cachexia under aging or heart failure conditions.

In zebrafish, *mstn* is expressed in several organs such as gill, brain, eye, and heart [12], however its function has only been characterized in skeletal muscle using different approaches. For instance, a transgenic line expressing the *mstn* prodomain driven by the light chain myosin (*mylc*) promoter showed hyperplasia of muscle fibres [13]. Later, dsRNA was used to target the active peptide region, obtaining the double muscle phenotype [14]. Also, a vector-based antisense RNA was used to silence *mstn* [15] resulting in hypertrophy and hyperplasia in skeletal muscle, as well as increased expression levels of myogenic factors. Here, in order to study *mstn* function in cardiac muscle, the CRISPR/Cas9 nuclease system [16,17] was used to inactivate *mstn* in zebrafish.

MATERIALS AND METHODS

Construction of the CRISPR/Cas9 system and microinjection

A hybrid strain of zebrafish brood stock (TAB-WIK) was maintained in a re-circulating system. Embryos were obtained and raised according to [18,19].

The target sequence was designed from exon 3 (GenBank accession no. **AY323521.1**), corresponding to the sequence encoding the active peptide. The gRNA was synthesized according to [20]. Two partially overlapping oligonucleotides were designed to produce the template to synthesize the gRNA. Oligonucleotide 1 consisted of a T7 promoter (bold), the PAM site (underlined), 20 nucleotides corresponding to the target sequence (in parenthesis) and a generic gRNA sequence:

5 - **T A A T A C G A C T C A C T A T A** - N G G - (AGGGCCCAAAACGAATCCGG)-*GTTTTAGAGCTAGAAATAGC*-3'

Oligonucleotide 1 was annealed with oligonucleotide 2, which consisted of 80 nucleotides overlapping the generic gRNA sequence in oligonucleotide 1:

5'-AAAAGCACCGACTCGGTGCCACTTTTTCAAGTTGATAACGGACTAGCCTTA TTTTAACTT*GCTATTTCTAGCTCTAAAAC3*'

Both oligonucleotides were annealed in the overlapping regions (represented in italics) and the 3'-ends were extended using *Pfu* polymerase under the following conditions: 98°C 2 min, 50°C 10 min, and 72°C 10 min. The resulting double stranded DNA was used as template for *in vitro* transcription of the gRNA using the HiScribe T7 kit (New England Biolabs), following the manufacturer's instructions.

To synthesize the Cas9 mRNA, a pT3TS-nCas9n plasmid was obtained from Addgene (plasmid #46757), and was processed according to the CRISPR plasmid protocol from [21]. The plasmid was linearized and used as template for *in vitro* transcription of the Cas9 mRNA using the mMESSAGEmMACHINE T3® kit (Ambion) following the instructions provided by the manufacturer.

The injection mix consisted of gRNA, Cas9 mRNA, phenol red (final concentration 0.01%), and nuclease-free water. Experimental groups were separated as follows: embryos injected with myostatingRNA (*mstn*, n=158), embryos injected with the mix without gRNA (n=43), and non-injected embryos (n=38). The mix was injected to each embryo using a PV 820 Pneumatic PicoPump (World Precision Instruments) microinjector.

Heart rate recording and sampling

The heartbeat of embryos at 2 dpf was recorded for 30 seconds using as CMOSpco. Edge high resolution video camera coupled to an Olympus BX51WI microscope with a magnification of 20X. At this stage the cardiovascular system is developed, embryos are transparent, static and easy to handle. At 5 dpf fish were anesthetized with 4% MESAB (MS-222) for sampling. The posterior region was preserved in absolute ethanol for DNA extraction [22] and the anterior region was preserved in 4% formalin for histology.

Histological analysis

Serial coronal sections were obtained from 5 dpf larvae, and stained with haematoxylin-eosin. The area of five muscle fibres per larvae were captured (Qimaging Micro Publisher coupled to an Olympus CX41 light microscope) and measured (SigmaScanPro 5.0 software). The heart was carefully observed looking for morphological differences between mutant and normal fish.

Genotyping by NGS

The region containing the target sequence was amplified using the Zf-mst1-F and Zf-mst1-R primers rendering a product of about 900 bp (Table 1, Figure 1). Then nested PCR reactions were performed using a set of four M13 forward primers, each one with a different barcode: M13-1-Zf_mst1-F to M13-4-Zf_mst1-F, and one M13 reverse primer (M13 - Zf_mst1-R), rendering a product of about 100 bp (Table 1, Figure 1). Final PCR reactions were carried out using IonXpress with different barcode sequences; the reverse primer was RVS for all reactions (Table 2, Figure 1).

Once the three PCR reactions were completed, all samples were pooled together and purified using the Wizard® SV Gel and PCR Clean-Up System (Promega), followed by an additional step with AMPure-XP® paramagnetic beads (Beckman Coulter). These barcode libraries were sequenced using a 316 chip and the Hi-Q sequencing chemistry on the Ion Torrent PGM (Thermo Fisher Scientific). The sequencing reads were retrieved as FASTQ and demultiplexed based on the combinatorial barcodes in both IonXpress and M13-Zf-mst-1 primers used in the third and second PCRs, respectively. A strict quality-filter of Q < 20 (Phred score) in any position was then applied, obtaining an average of 341 clean reads per individual. Sequences from each individual were transformed to FASTA, aligned against the wild type reference sequence and compared.

RESULTS AND DISCUSSION

Mortality was 80% for the *mstn* group, 35% for the injected control group, and 5% for the non-injected control group indicating that some mortality was due to both the microinjection and the mutation. The mutation success was 90.6%. From the 29 mutant fish, a total of 9024 sequences were analysed, with an average of 334 sequences per individual. Mutations were classified into different types, depending on the number of inserted or deleted nucleotides (Figure 2). Indel range was consistent with previous reports using the CRISPR/Cas9 nuclease system in zebrafish [21].

Significant differences in skeletal muscle fibre area were observed in 5 dpf larvae as shown in (Figure 3A, 3B) (Kluskal-Wallis analysis of variance followed by paired Dunn comparisons; P < 0.001). This phenotype is consistent with previous reports [13-15], confirming that the inactivation of *mstn* was successful. No evident histological alterations between mutant and control larvae were observed in the heart (Figure 3C). Nevertheless, the mutation did produce a reduction in the heart rate. The number of heart beats per minute in 2 dpf embryos are shown in Figure (4). Significant differences were found between mutant and con-

Table 1: Primer sequences used in the first (Zf-mst1-F and Zf-mst1-R) and second (M13-1-Zf_mst1-F to M13-4-Zf_mst1-F, and M13 – Zf_mst1-R) PCR reactions. Barcode sequences are underlined.

Primer name	*Sequence (5´- 3´)*
Zf-mst1-F	ACC CCT CAA CCA TTG GGT TC
Zf-mst1-R	AGT CGC ATT CTC CTG AAC AGT
M13_1-Zf_mst1-F	GTA AAA CGA CGG CCA GCT AAG GTA AC C AGC TCC CCT TTA TGG AGGT
M13_2-Zf_mst1-F	GTA AAA CGA CGG CCA GTA AGG AGA ACC AGC TCC CCT TTA TGG AGG T
M13_3-Zf_mst1-F	GTA AAA CGA CGG CCA GAA GAG GAT TCC AGC TCC CCT TTA TGG AGG T
M13_4-Zf_mst1-F	GTA AAA CGA CGG CCA GTA CCA AGA TCC AGC TCC CCT TTA TGG AGG T
M13 - Zf_mst1-R	CAG GAA ACA GCT ATG ACG CAG CGA GAC TCT GAG GAA T

Table 2: IonXpress primer sequences 17 to 32 (with barcode sequences underlined) used in the third PCR reaction set.

Primer	*Sequence (5´- 3´)*
IonXpress_17	CCA TCT CAT CCC TGC GTG TCT CCG ACT CAG TCT ATT CGT CGA TGT AAA ACG ACG GCC AG
IonXpress_18	CCA TCT CAT CCC TGC GTG TCT CCG ACT CAG AGG CAA TTG CGA TGT AAA ACG ACG GCC AG
IonXpress_19	CCA TCT CAT CCC TGC GTG TCT CCG ACT CAG TTA GTC GGA CGA TGT AAA ACG ACG GCC AG
IonXpress_20	CCA TCT CAT CCC TGC GTG TCT CCG ACT CAG CAG ATC CAT CGA TGT AAA ACG ACG GCC AG
IonXpress_21	CCA TCT CAT CCC TGC GTG TCT CCG ACT CAG TCG CAA TTA CGA TGT AAA ACG ACG GCC AG
IonXpress_22	CCA TCT CAT CCC TGC GTG TCT CCG ACT CAG TTC GAG ACG CGA TGT AAA ACG ACG GCC AG
IonXpress_23	CCA TCT CAT CCC TGC GTG TCT CCG ACT CAG TGC CAC GAACGA TGT AAA ACG ACG GCC AG
IonXpress_24	CCA TCT CAT CCC TGC GTG TCT CCG ACT CAG AAC CTC ATT CGA TGT AAA ACG ACG GCC AG
IonXpress_25	CCA TCT CAT CCC TGC GTG TCT CCG ACT CAG CCT GAG ATA CGA TGT AAA ACG ACG GCC AG
IonXpress_26	CCA TCT CAT CCC TGC GTG TCT CCG ACT CAG TTA CAA CCT CGA TGT AAA ACG ACG GCC AG
IonXpress_27	CCA TCT CAT CCC TGC GTG TCT CCG ACT CAG AAC CAT CCGCGA TGT AAA ACG ACG GCC AG
IonXpress_28	CCA TCT CAT CCC TGC GTG TCT CCG ACT CAG ATC CGG AATCGA TGT AAA ACG ACG GCC AG
IonXpress_29	CCA TCT CAT CCC TGC GTG TCT CCG ACT CAG TCG ACC ACTCGA TGT AAA ACG ACG GCC AG
IonXpress_30	CCA TCT CAT CCC TGC GTG TCT CCG ACT CAG CGA GGT TAT CGA TGT AAA ACG ACG GCC AG
IonXpress_31	CCA TCT CAT CCC TGC GTG TCT CCG ACT CAG TCC AAG CTGCGA TGT AAA ACG ACG GCC AG
IonXpress_32	CCA TCT CAT CCC TGC GTG TCT CCG ACT CAG TCT TAC ACA CGA TGT AAA ACG ACG GCC AG
RVS_primer	CCT CTC TAT GGG CAG TCG GTG ATC AGG AAA CAG CTA TGA C

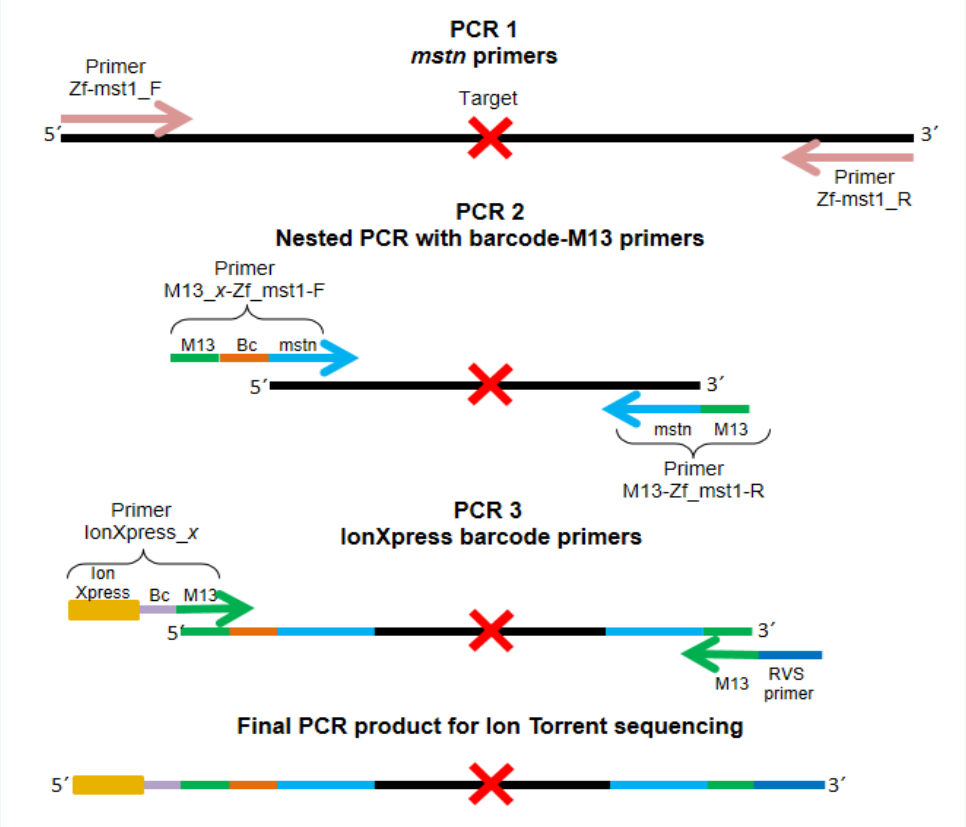

Figure 1 Multiplex adapter tailing strategy. Genome edits produced by CRISPR/Cas9 were characterized by NGS. Barcode libraries were generated by three consecutive PCR reactions. The first reaction was used to amplify the target site (PCR1), the second nested PCR reaction was used to introduce four different barcodes coupled to M13 sequences (PCR2), and the third PCR reaction was used to introduce more barcodes and the IonXpress adaptors for NGS. Primers are indicated: *M13 (1 – 4)-Zf_mst1-F*: M13 tail (M13), specific barcode (Bc), and *mstn* recognition site (mst1). *M13-Zf_mst1-R*: *mstn* recognition site (mst1) and M13 tail (M13). *IonXpress (17 – 32)*: adapter (IonXpress), specific barcode (Bc), and M13 tail (M13). *RVS primer*: M13 tail (M13) and reverse primer.

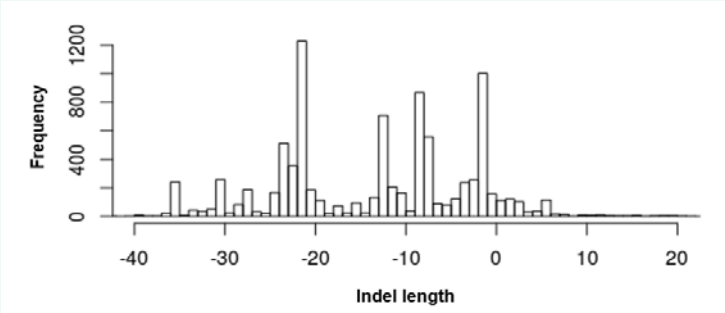

Figure 2 Types of mutations (indels) obtained after genomic edition with CRISPR/Cas9. From the 9024 sequences obtained from the 29 fish, only 2% (n=156) did not show indels. Deletions (negative numbers) of 21 nucleotides were the most frequent (n=1227, 14%), followed by deletions of 1 nucleotide (n=1002, 11%), deletions of 8 nucleotides (n=867, 10%), and deletions of 12 nucleotides (n=707, 8%). Insertions (positive numbers) occurred in lower proportions: 2 nucleotides (n=120, 1.33%), 6 nucleotides (n=114, 1.26%), 1 nucleotide (n=111, 1.23%), and 3 nucleotides (n=102, 1.13%).

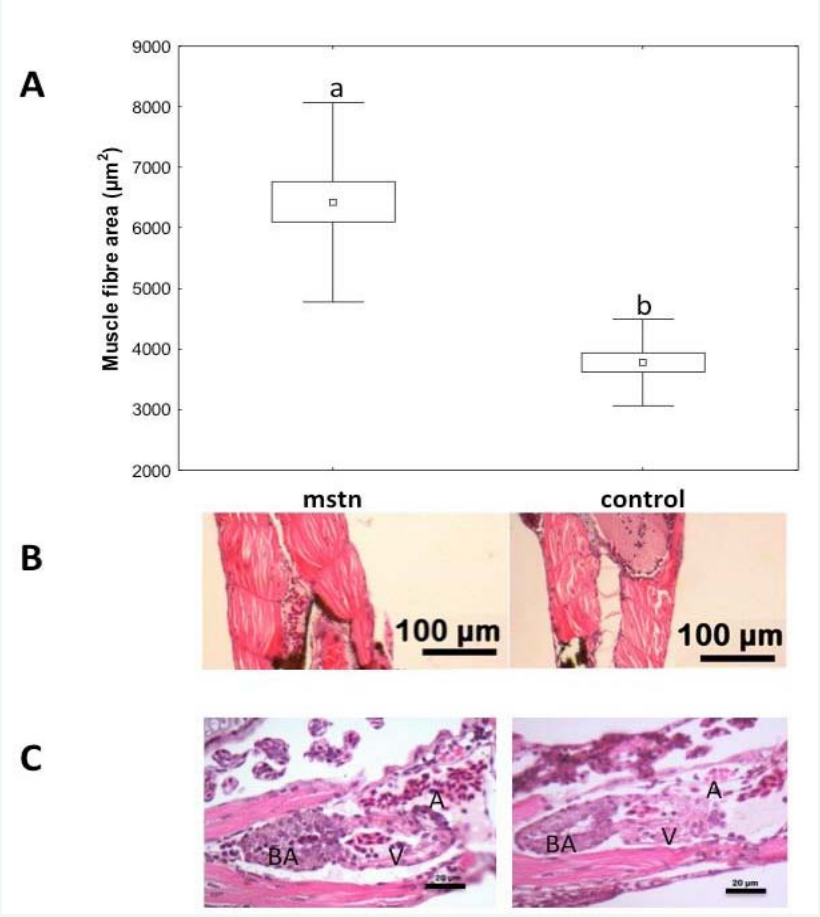

Figure 3 A) Muscle fibre area and B) coronal histological sections of skeletal muscle from 5 dpf larvae injected with *mstn* gRNA (n=7) and the control group (n=4). Because of the low number of 5 dpf larvae in coronal orientation, the control group includes both injected and non-injected groups. Five muscle fibres were measured per larvae. The dot represents the mean, the box represents the standard error, and the bars the standard deviation. Different letters indicate significant differences in muscle fibre size (P<0.001). C) Coronal histological sections of the heart of 5 dpf larvae. The scale bar represents 20μm. BA-bulbus arteriosus; V-ventricle; A-atrium.

trol embryos (Kluskal-Wallis analysis of variance followed by paired Dunn comparisons; $P < 0.001$).

Results regarding the role of myostatin in heart size and ventricular hypertrophy using mouse models are scarce and contradictory [4,6-9]. Interestingly, a significant decrease of systolic contractions in *mstn*-null mice in resting state has been reported [4]. This is important because de inhibition of *mstn* seems to improve heart performance in aging mammalian models [7] prob-

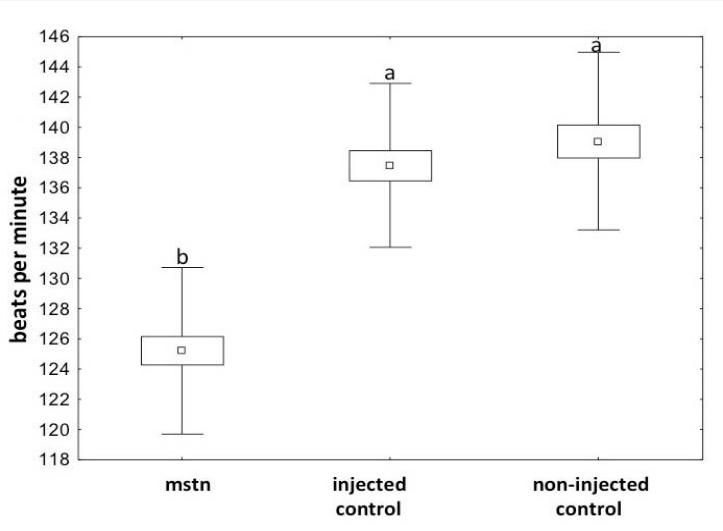

Figure 4 Cardiac rate (beats per minute) from 2 dpf embryos (n=24 for the *mstn*-mutant group, n=23 for the injected control group, n=29 for the non-injected control group). The dot represents the mean, the box represents the standard error, and the bars the standard deviation. Different letters indicate significant differences in the cardiac rate (P<0.001).

ably by reducing systolic contractions. Consistent with these observations, *mstn*-mutant zebrafish embryos presented a reduced cardiac beat rate in resting state, suggesting a role for myostatin as a modulator of cardiac function not only under heart failure or aging situations, but also during development.

CONCLUSION

Genomic edition of *mstn* in zebrafish embryos resulted in a significant reduction in the heart rate, suggesting that *mstn* could play a role in the regulation of cardiac contractions during embryonic development.

ACKNOWLEDGEMENTS

The authors would like to thank the Laboratory of Cellular and Molecular Neurobiology (UNAM) for microinjection facilities. Thanks to Rubí Hernandez-Cornejo for technical assistance; to Bruno Gómez-Gil and JulissaEnciso for barcode-library sequencing; to ItzelSifuentes-Romero, Juan Manuel Martínez-Brown, and Cristina Chávez-Sánchez for constructive comments to this work. This work was supported by the National Council for Science and Technology (CONACYT) (grant CB-179098).

REFERENCES

1. Thomas M, Langley B, Berry C, Sharma M, Kirk S, Bass J, et al. Myostatin a negative regulator of muscle growth, functions by inhibiting myoblast proliferation. J Biol Chem. 2000; 275: 40235-41243.
2. McPherron A, Lee SJ. Double muscling in cattle due to mutations in the myostatin gene. Proc Natl Acad Sci U S A. 1997; 94: 12457-12461.
3. Kambadur R, Sharma M, Smith TP, Bass JJ. Mutations in myostatin (GDF8) in double-muscled Belgian blue and piedmontese cattle. Genome Res. 1997; 7: 910-916.
4. Rodgers BD, Interlichia JP, Garikipati DK, Mamidi R, Chandra M, Nelson OL, et al. Myostatin represses physiological hypertrophy of the heart and excitation-contraction coupling. J Physiol. 2009; 587: 4873-4886.
5. Ciarmela P, Wiater E, Smith SM, Vale W. Presence, actions, and regulation of myostatin in rat uterus and myometrial cells. Endocrinology. 2009; 150: 906-914.
6. Morissette MR, Cook SA, Foo S, McKoy G, Ashida N, Novikov M, et al. Myostatin regulates cardiomyocyte growth through modulation of Akt signaling. Circ Res. 2006; 99: 15-24.
7. Morissette MR, Stricker JC, Rosenberg MA, Buranasombati C, Levitan EB, Mittleman MA , et al. Effects of myostatin deletion in aging mice. Aging Cell. 2009; 8: 573-583.
8. Artaza JN, Reisz-Porszasz S, Dow JS, Kloner RA, Tsao J, Bhasin S, et al. Alterations in myostatin expression are associated with changes in cardiac left ventricular mass but not ejection fraction in the mouse. J Endocrinol. 2007; 194: 63-76.
9. Cohn RD, Liang HY, Shetty R, Abraham T, Wagner KR. Myostatin does not regulate cardiac hypertrophy or fibrosis. Neuromuscul Disord. 2007; 17: 290-296.
10. Silljé HH, de Boer RA. Myostatin: an overlooked player in heart failure. Eur J Heart Fail. 2010; 12: 420-422.
11. Heineke J, Auger-Messier M, Xu J, Sargent M, York A, Welle S, et al. Genetic deletion of myostatin from the heart prevents skeletal muscle atrophy in heart failure. Circulation. 2010; 121: 419-425.
12. Helterline DL, Garikipati D, Stenkamp DL, Rodgers BD. Embryonic and tissue-specific regulation of myostatin-1 and -2 gene expression in zebrafish. Gen Comp Endocrinol. 2007; 151: 90-97.
13. Xu C, Wu G, Zohar Y, Du SJ. Analysis of myostatin gene structure, expression and function in zebrafish. J Exp Biol. 2003; 206: 4067-4079.
14. Acosta J, Carpio Y, Borroto I, González O, Estrada MP. Myostatin gene silenced by RNAi show a zebrafish giant phenotype. J Biotechnol. 2005; 119: 324-331.
15. Lee C-Y, Hu S-Y, Gong H-Y, Chen MH-C, Lu J-K, Wu J-L. Suppression of myostatin with vector-based RNA interference causes a double-muscle effect in transgenic zebrafish. Biochem Biophys Res Commun. 2009; 387: 766-771.
16. Hruscha A, Krawitz P, Rechenberg A, Heinrich V, Hecht J, Haass C, et al. Efficient CRISPR/Cas9 genome editing with low off-target effects in zebrafish. Development. 2013; 140: 4982-4987.

17. Hwang WY, Fu Y, Reyon D, Maeder ML, Tsai SQ, Sander JD, et al. Efficient genome editing in zebrafish using a CRISPR-Cas system. Nature Biotechnol. 2013; 31: 227-229.

18. Matthews M, Trevarrow B, Matthews J. A virtual tour of the Guide for zebrafish users. Lab Anim (NY). 2002; 31: 34-40.

19. Best J, Adatto I, Cockington J, James A, Lawrence C. A novel method for rearing first-feeding larval zebrafish: polyculture with Type L saltwater rotifers (Brachionus plicatilis). Zebrafish. 2010; 7: 289-295.

20. Varshney GK, Pei W, LaFave MC, Idol J, Xu L, Gallardo V, et al. High-throughput gene targeting and phenotyping in zebrafish using CRISPR/Cas9. Genome Res. 2015; 25: 1030-1042.

21. Jao LE, Wente SR, Chen W. Efficient multiplex biallelic zebrafish genome editing using a CRISPR nuclease system. Proc Natl Acad Sci U S A. 2013; 1100: 13904-13909.

22. Miller SA, Dykes DD, Polesky HF. A simple salting out procedure for extracting DNA from human nucleated cells. Nucleic Acids Res. 1988; 16: 1215.

Cite this article

Lizárraga-Lizárraga D, Martínez-Torres A, Llera-Herrera R, Espino-Saldaña ÁE, García-Gasca A (2017) Myostatin Modulates the Heart Rate in Zebrafish Embryos. JSM Biotechnol Bioeng 4(1): 1077.